

HIGH-RESOLUTION ELECTRON ENERGY-LOSS SPECTROSCOPY (HREELS) USING A MONOCHROMATED TEM/STEM. Z. R. Dai^{1*}, J. P. Bradley^{1*}, R. Erni^{2,3} and N. Browning^{2,3}, ¹Institute of Geophysics and Planetary Physics, Lawrence Livermore National Laboratory, Livermore CA 94551, ³ Dept. of Chemical Engineering and Materials Science, UC Davis, Davis, CA 95616, ³National Center for Electron Microscopy, Lawrence Berkeley National Laboratory, Berkeley CA 94551, *Bay Area Particle Analysis Consortium (BAYPAC).

Introduction: A 200 keV FEI TF20 XT monochromated (scanning) transmission electron microscope funded by NASA's SRLIDAP program is undergoing installation at Lawrence Livermore National Laboratory. Instrument specifications in STEM mode are Cs =1.0 mm, Cc =1.2 mm, image resolution =0.18 nm, and in TEM mode Cs =1.3 mm, Cc =1.3 mm, information limit =0.14 nm. Key features of the instrument are a voltage-stabilized high tension (HT) supply, a monochromator, a high-resolution electron energy-loss spectrometer/energy filter, a high-resolution annular dark-field detector, and a solid-state x-ray energy-dispersive spectrometer. The high-tension tank contains additional sections for 60Hz and high frequency filtering, resulting in an operating voltage of 200 kV \pm 0.005V, a >10-fold improvement over earlier systems. The monochromator is a single Wien filter design. The energy filter is a Gatan model 866 Tridiem-ERS high-resolution GIF spec'd for \leq 0.15 eV energy resolution with 29 pA of current in a 2 nm diameter probe. 0.13 eV has already been achieved during early installation (Fig. 1). The x-ray detector (EDAX/Genesis 4000) has a take-off angle of 20°, an active area of 30 mm², and a solid angle of 0.3 steradians. The higher solid angle is possible because the objective pole-piece allows the detector to be positioned as close as 9.47 mm from the specimen.

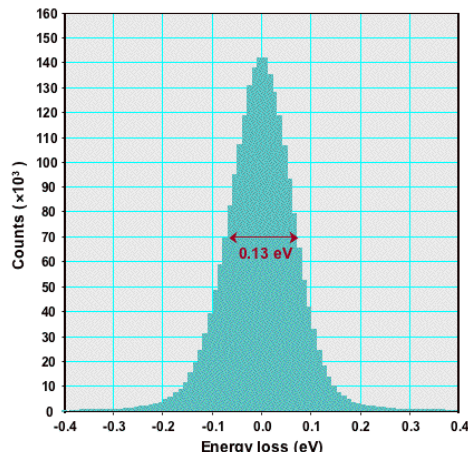


Figure 1: 200 keV zero-loss peak with monochromator on (Tecnai TF20 at LLNL). Energy resolution is 0.13 eV (FWHM) with an acquisition time of 1 second.

The voltage-stabilized HT supply, monochromator and GIF enable high-resolution electron energy-loss spectroscopy (HREELS) with energy resolution comparable to synchrotron XANES, but with ~100X better spatial resolution. The region between 0 and 100 eV is called the low-loss or valence electron energy-loss spectroscopy (VEELS) region where features due to collective plasma oscillations and single electron transitions of valence electrons are observed [1]. Most of the low-loss VEELS features we are detecting are being observed for the first time in IDPs (Fig. 2). A major focus of our research is to understand the origin and significance of these features and how they might be exploited to gain insight about IDPs and other meteoritic materials.

Figure 2 compares HREELS spectra from a fluid inclusion within glass and from the glass itself in IDP W7013E-17 [2]. Reference spectra from gaseous O₂ and amorphous ice are also plotted. In addition to the main volume plasmon (K), the fluid inclusion spectrum (red) has at least ten other edges (labeled A-J).

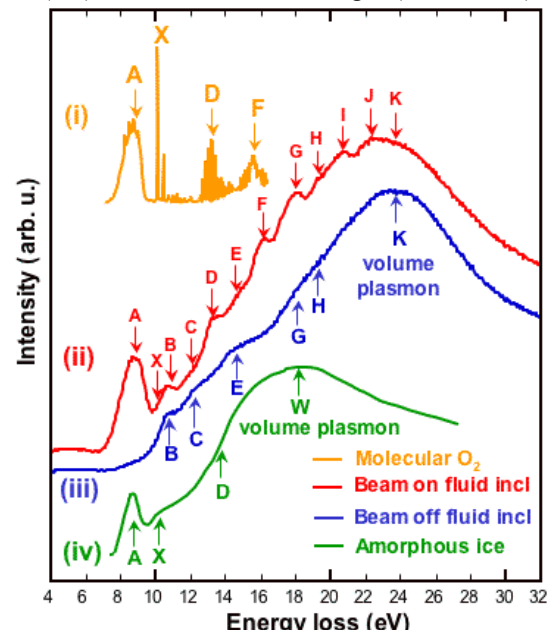


Figure 2: Energy-loss spectra from (i) O₂ gas [3], (ii) ~ 10 nm diameter fluid inclusion within aluminosilicate glass in IDP W7013E-17, (iii) glass matrix alongside fluid inclusion, (iv) amorphous ice [4].

When the electron probe is moved off the fluid inclusion (Fig. 2, blue) only edges B, C, E, G, H and K remain, although G and H are much weaker. B, C, E & G are due to SiO_4^{-4} excitons, H is a surface plasmon and K is the energy maximum of the volume plasmon.

A, D, F, I and J are specific to the fluid inclusion. "A" correlates with a pre-edge on the oxygen-K feature at ~ 532 eV. Comparison with the O_2 spectrum (Fig. 2, orange) suggests that the feature may be due to O_2 gas, although the intense O_2 "X" peaks show up only faintly in the fluid inclusion. Since amorphous ice also gives a strong "A" feature (Fig. 2, green), the fluid inclusion "A" feature could also be due to -OH, -OOH, peroxide, etc. The I and J edges from the fluid inclusion may be related to A, although it is intriguing that the position of J (~ 22 eV) is consistent with the Helium $1s \rightarrow 2p$ core excitation edge. Time-resolved *in-situ* observations indicate that the intensities of edges A, D, F, I, and J decrease as the contents of the fluid inclusion are released as the glass degrades and fluid inclusion perforates under electron irradiation (Fig. 3).

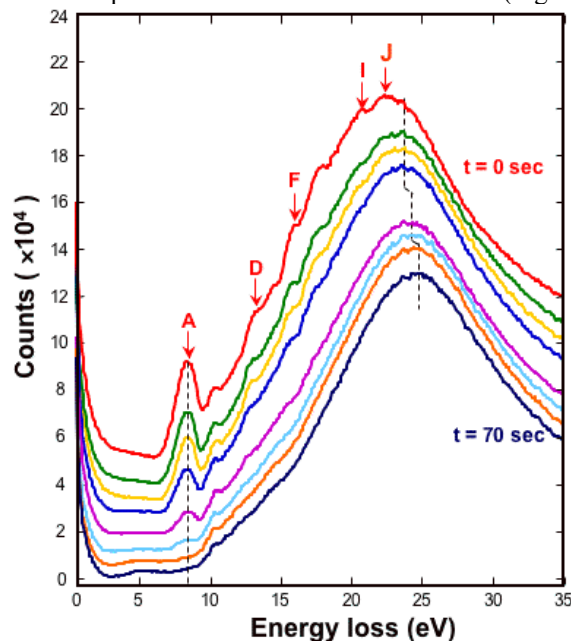


Figure 3: Time-resolved HREELS spectra from a fluid inclusion in IDP W7013E-17.

We have compared the UV spectral properties of IDPs with those of dust in the interstellar medium (Fig. 4) [5]. The 1-10 eV VEELS region corresponds to the 1241-124 nm visible/ultraviolet wavelength region, although VEELS offers $\sim 10X$ less energy/wavelength resolution than photo-absorption spectroscopy [6]. The 2175 Å extinction feature is by far the strongest UV-VIS spectral signature of interstellar dust observed by astronomers. Forty years after its discovery the origin of the feature and the nature of the carrier remain controversial. We have identified carriers of a 2175 Å

feature in chondritic IDPs. The carrier grains are organic carbonaceous matter and GEMS, some with non-solar isotopic compositions confirming that they are interstellar grains.

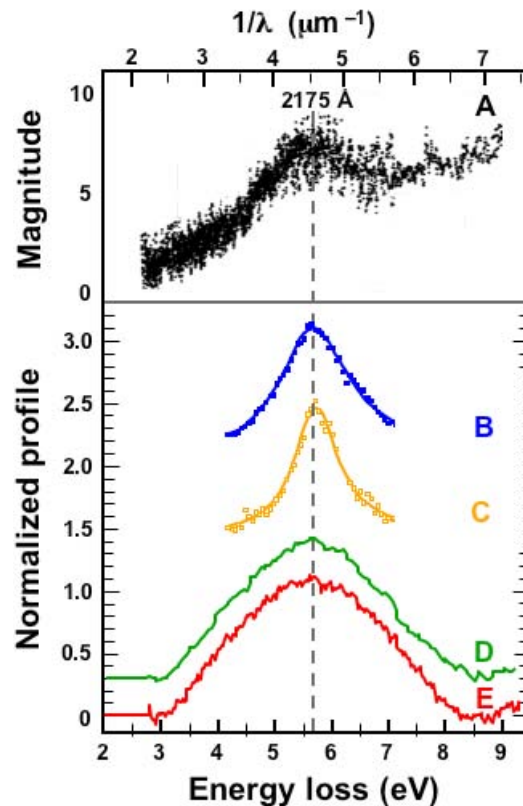


Figure 4: Comparison of astronomical UV extinction features with laboratory UV/VEELS features. (A) The 2175 Å interstellar extinction feature from two stars ζ and ϵ Persei [7]. (B) Broadest (ζ Oph) and (C) narrowest (HD 93028) profiles from 45 stars [8]. (D) VEELS spectrum from (organic) carbon in IDP L2047 D23. (E) VEELS spectrum from GEMS in W7013 E17.

References: [1] Dorneich, A. D. et al (1998) *J. Microsc.* 191, 286-296. [2] Erni, R. et al (2005) *Micron* (in press). [3] York T.A. and Comer J. (1983) *J. Phys. B: At. Mol. Phys.* 16, 3627-3639. [4] Leapman R.D. and Sun S. (1995) *Ultramicroscopy* 59, 71-79. [5] Bradley, J. P. et al. (2005) *Science*, in press (Jan. 14 issue, 2005). [6] Brion, C. E. et al (1982) *AIP Conf. Proc. No. 94*, 429-446. [7] Stecher, T. P. (1969) *Ap. J.* L125-L126. [8] Fitzpatrick, E. L. and Massa, D. (1986) *Ap. J.* 307, 286-294.

Acknowledgement: This research is supported by NASA grants NAG5-7450, NAG5-10632 and NAG10696. This work was also performed under the auspices of the US Dept. of Energy by the Lawrence Livermore National Laboratory under contract No. W-7405-ENG-48.